ISSN 0006-2979, Biochemistry (Moscow), 2007, Vol. 72, No. 5, pp. 518-528. © Pleiades Publishing, Ltd., 2007.
Original Russian Text © A. V. Meremyanin, T. B. Eronina, N. A. Chebotareva, S. Yu. Kleimenov, I. K. Yudin, K. O. Muranov, M. A. Ostrovsky, B. I. Kurganov, 2007, published in Biokhimiya, 2007, Vol. 72, No. 5, pp. 642-654.

Effect of α-Crystallin on Thermal Aggregation of Glycogen Phosphorylase *b* from Rabbit Skeletal Muscle

A. V. Meremyanin[1]*, T. B. Eronina[1], N. A. Chebotareva[1], S. Yu. Kleimenov[1], I. K. Yudin[2], K. O. Muranov[3], M. A. Ostrovsky[3], and B. I. Kurganov[1]

[1]*Bach Institute of Biochemistry, Russian Academy of Sciences, Leninsky pr. 33, 119071 Moscow, Russia; fax: (495) 954-2732; E-mail: mer-av@inbi.ras.ru*
[2]*Oil and Gas Research Institute, Russian Academy of Sciences, ul. Gubkina 3, 119991 Moscow, Russia*
[3]*Emanuel Institute of Biochemical Physics, Russian Academy of Sciences, ul. Kosygina 4, 117997 Moscow, Russia*

Received December 27, 2006

Abstract—Thermal aggregation of rabbit skeletal muscle glycogen phosphorylase *b* (Ph*b*) has been investigated using dynamic light scattering under conditions of a constant rate of temperature increase (1 K/min). The linear behavior of the dependence of the hydrodynamic radius on temperature for Ph*b* aggregation is consistent with the idea that thermal aggregation of proteins proceeds in the kinetic regime wherein the rate of aggregation is limited by diffusion of the interacting particles (the regime of "diffusion-limited cluster–cluster aggregation"). In the presence of α-crystallin, a protein exhibiting chaperone-like activity, the dependence of the hydrodynamic radius on temperature follows the exponential law; this suggests that the aggregation process proceeds in the kinetic regime where the sticking probability for colliding particles becomes lower than unity (the regime of "reaction-limited cluster–cluster aggregation"). Based on analysis of the ratio between the light scattering intensity and the hydrodynamic radius of Ph*b* aggregates, it has been concluded that the addition of α-crystallin results in formation of smaller size starting aggregates. The data on differential scanning calorimetry indicate that α-crystallin interacts with the intermediates of the unfolding process of the Ph*b* molecule. The proposed scheme of thermal denaturation and aggregation of Ph*b* includes the stage of reversible dissociation of dimers of Ph*b* into monomers, the stage of the formation of the starting aggregates from the denatured monomers of Ph*b*, and the stage of the sticking of the starting aggregates and higher order aggregates. Dissociation of Ph*b* dimer into monomers at elevated temperatures has been confirmed by analytical ultracentrifugation.

DOI: 10.1134/S0006297907050082

Key words: glycogen phosphorylase *b*, denaturation, aggregation, α-crystallin, dynamic light scattering, analytical ultracentrifugation

Formation of insoluble intracellular aggregates due to protein misfolding is a common pathogenetic basis for many degenerative and human neurodegenerative diseases including Alzheimer's, Parkinson's, Huntington's, and other diseases [1, 2]. Heat shock proteins (HSPs) playing the role of molecular chaperones [3] and found in all organisms [4], can prevent protein aggregation. Human and animal lens protein, crystallin, is also an HSP. Like other HSPs, it does not exhibit specificity with respect to protein substrates, and αB-crystallin has been found in almost all tissues, including skeletal muscle [5]. *In vitro* α-crystallin suppressed aggregation of a number of proteins [6-8]. It is suggested that α-crystallin suppression of aggregation of denatured proteins involves its binding to hydrophobic sites of a nonnative protein; increase in temperature increased this ability [9, 10]. The three-dimensional structure of α-crystallin still remains unknown due to its polydispersity and also due to variations of oligomeric state and molecular mass, which may vary depending on temperature and isolation conditions of this protein [11].

In this study, we have investigated the effect of α-crystallin on thermal aggregation of glycogen phosphorylase *b* (Ph*b*). Glycogen phosphorylase (1,4-α-D-glucan:orthophosphate-α-D-glycosyl transferase; EC 2.4.1.1) is the key enzyme of glycogen metabolism in skeletal muscles. Ph*b* catalyzes the first stage of glycogen degradation. In a resting muscle, the enzyme exists in the

Abbreviations: DSC) differentiation scanning calorimetry; Ph*b*) glycogen phosphorylase *b*; HSP) heat shock protein.

* To whom correspondence should be addressed.

nonphosphorylated form (*b* form), which is inactive in the absence of AMP. Ph*b* is an oligomeric enzyme; it is a dimer, which consists of two identical subunits with molecular mass of 97.4 kD [12]. Earlier we studied thermal denaturation [13-15] and chemical denaturation of Ph*b* induced by guanidine hydrochloride [16, 17]. It was found that the denaturation process includes a stage of conformation changes of the dimeric form of Ph*b* and a stage of reversible dissociation of the enzyme dimer to monomers followed by monomer unfolding.

In the previous studies [8, 18, 19], we proposed a new mechanism of thermal protein aggregation leading to amorphous aggregate formation. The proposed mechanism includes the stage of formation of starting aggregates (primary clusters) followed by the subsequent stages of sticking of the starting aggregates and higher order aggregates. Within the framework of this mechanism the effect of α-crystallin was explained by formation of smaller-sized starting aggregates and decreased sticking probability of the interacting particles during their collision.

In this present study, we have demonstrated applicability of this mechanism of chaperone-like activity of α-crystallin for thermal aggregation of Ph*b*. Thermal aggregation of Ph*b* in the absence and the presence of α-crystallin was investigated under the conditions of a constant rate of temperature increase. A similar approach has recently been employed for studies of the protecting effect of α-crystallin during aggregation of rabbit skeletal muscle glyceraldehyde-3-phosphate dehydrogenase [20].

Denaturation of Ph*b* was monitored by differential scanning calorimetry; using this method, it was possible to compare denaturation and aggregation under identical conditions. Special interest in Ph*b* is determined by the fact that thermal enzyme denaturation follows a dissociative mechanism and includes a stage of reversible dissociation of dimers into monomers [13-15].

MATERIALS AND METHODS

Hepes, EDTA, and NaCl used in this study were purchased from Reakhim (Russia). Bovine lens α-crystallin was isolated and purified using methods described earlier [18, 21].

Rabbit skeletal muscle Ph*b* was isolated by the method of Fisher and Krebs [22], using dithiothreitol instead of cysteine and triple recrystallization of the enzyme. Concentrations of Ph*b* and α-crystallin were determined spectrophotometrically at 280 nm using absorbance coefficient of 13.2 and 8.5 for 1% solution of Ph*b* [23] and α-crystallin [24], respectively.

Thermal denaturation of Ph*b* and α-crystallin and a mixture of these proteins was investigated by differentiation scanning calorimetry (DSC) using the adiabatic scanning microcalorimeter DASM-4M (Institute of Biological Instruments, Russian Academy of Sciences, Pushchino, Russia) with 0.47-ml capillary platinum cells [25]. All measurements were carried out in 0.08 M Hepes buffer, pH 6.8, containing 0.2 mM EDTA and 0.1 M NaCl at the rate of heating of 1 K/min using the temperature range from 20 to 85°C and constant pressure of 2.2 atm. The dependence of excess heat capacity versus temperature was calculated using the program Origin (MicroCal, Inc, USA).

The kinetics of Ph*b* aggregation in 0.08 M Hepes buffer, pH 6.8, containing 0.2 mM EDTA and 0.1 M NaCl, in the absence and in the presence of α-crystallin was investigated by dynamic light scattering; this method allows the real-time detection of sizes of forming aggregates to be evaluated [26]. The method is based on measurements of statistical characteristics of light scattered due to fluctuations of particle concentrations in a given volume. Characteristic relaxation time τ_c can be found using the correlation function of fluctuations of scattered light intensity; it is linked to the diffusion coefficient of nanoparticles *D* (protein aggregation in this case) by the following expression:

$$D = \frac{1}{2\tau_c k^2}, \qquad k = \frac{2\pi n}{\lambda}\sin\frac{\theta}{2}, \tag{1}$$

where *k* is the wave vector of scattered light, *n* is solvent refractive index, λ is wavelength of incident light, and θ is the scattering angle. The hydrodynamic radius of particles, *R*, can then be calculated using the Stokes–Einstein formula:

$$D = \frac{k_B T}{6\pi\eta R}, \tag{2}$$

where k_B is the Boltzmann constant, *T* is temperature, and η is solvent viscosity.

It is important to emphasize that this interpretation of results from dynamic light scattering is applicable for the case of non-colliding particles. However, in the aggregation process particle collision definitely occurs. In this case, dynamic light scattering may be correctly employed for determination of average current size of particles, provided that characteristic aggregation time was much higher than the time required for measurement of each size particle. During measurements of aggregation kinetics, such time ratios are very important. In our case, this precondition was very reliable.

Kinetic studies of protein aggregation were carried out using a Photocor Complex instrument (Photocor Instruments, USA) with a He-Ne laser as a source of light (wavelength of 632.8 nm, maximum power of 15 mW). When necessary, laser power could be decreased to exclude parasite effects attributed to overheating of the investigated sample during absorbance of a part of the

incident energy. Measurements were carried out at the fixed scattered angle of 90°. The scattered light was accepted by a cross-correlation system for photon counting, which could detect particles of size ranging from 0.5 nm to 5 μm. Signals from the photon counting system were then analyzed by the Photocor-FC correlator using both linear and logarithmic time scale. The value of the integral intensity of light scattering was analyzed simultaneously with measurement of the correlation function of light scattered. Correlation functions were analyzed by means of the DYNALS program of polydisperse analysis (Alango, Israel).

It was also important to compare the results obtained by dynamic light scattering with the results obtained by DSC at high rates of temperature scanning. Since the standard Photocor Complex thermostat cannot provide the required scanning rates, we have developed a miniaturized low-inertia thermostat with temperature scanning rates up to 10°C/min. Temperature control error did not exceed 0.1°C. Increased accuracy of temperature measurements at high scanning rates was achieved by use of a special platinum thermometer, which was placed directly into the sample.

All solutions used were prepared using deionized water obtained from an Easy–Pure II RF system (Barnstead, USA). The aggregation reaction was initiated by adding Ph*b* solution (10-50 μl) to the buffer with or without α-crystallin thermostatted for 5 min. Total volume of the reaction mixture was 0.5 ml.

Velocity sedimentation experiments were carried out at 20 and 48°C using a Spinco analytical ultracentrifuge, model E (Beckman, USA) equipped with the absorption optical scanning system, a monochromator, and a computer. A four-channel titanium rotor An-F and 12-mm two-sector cells were used in experiments. During sedimentation studies at 48°C, the rotor was thermostatted overnight at this temperature. Sedimentation was registered by enzyme absorption at 280 nm. The interval between scannings was 3 min. All the cells were scanned simultaneously. For digitized data collection, we have used La-n20-12 PCI and La-1.5 PCI cards and the program developed by A. G. Zharov for these purposes (www.ADClab.ru). The sedimentation coefficients were determined from differential distributions of sedimentation coefficients [$c(s)$; s] or [$c(s, f/f_0)$; s] using the program SEDFIT [27, 28]. Mean values of the sedimentation coefficients of separate forms were obtained by integration of differential distribution peaks. Sedimentation coefficients were normalized to standard conditions (solvent with density and viscosity of water at 20°C) as described in [15].

Analysis of kinetic data on protein aggregation. Results of studies on kinetics of thermal protein aggregation using dynamic light scattering [8, 18, 19, 29] indicate that the aggregation process begins with the initial stage, known as the formation of starting aggregates. Their hydrodynamic radius (R_h) is about tens nanometers. Sticking of starting aggregates and then aggregates of higher order finally results in formation of large aggregates (R_h of 2000-4000 nm), which tend to precipitate. Thus, protein aggregates are highly disperse systems, which are studied by colloidal chemistry. Problems of stability of the colloidal systems and aggregation of particles with sizes 1-1000 nm have been well studied. Collisions result in formation of particle assemblies stabilized by surface forces [30, 31].

Two extreme kinetic regimes of colloidal particles aggregation have been identified. In the absence of distraction forces between particles, each collision results in sticking of the colliding particles. In this case, the rate of aggregation is limited by diffusion of colliding particles. This kinetic regime has been defined in the literature as a "diffusion-limited cluster–cluster aggregation" (DLCA). When probability of particle sticking is lower than unity another kinetic regime known as a "reaction-limited cluster–cluster aggregation" (RLCA) occurs. Transition of DLCA regime into RLCA regime is characterized by significant changes of the behavior of the time-dependence of hydrodynamic radius of particles (R_h). In the case of DLCA regime the initial part of the dependence of R_h versus time (t) is linear and can be described by the following linear dependence:

$$R_h = R_{h,0}\left[1+\frac{t}{t_{2R}}\right], \qquad (3)$$

where $R_{h,0}$ is hydrodynamic radius of initial particles involved in aggregation and t_{2R} is time interval required for the hydrodynamic radius to reach the value of $2R_{h,0}$. The parameter t_{2R} characterizes the rate of the aggregation process. The greater the t_{2R} value is the less the aggregation rate.

When the time interval exceeds certain limit ($t > t^*$) the time dependence of R_h is described by a function of degree [32-35]:

$$R_h = R_h^*[1+K_1(t-t^*)]^{1/d_f}, \qquad (4)$$

where R_h^* is R_h value at $t = t^*$, K_1 is a constant, and d_f is a fractal dimension of aggregates. The fractal dimension is a structural characteristic of aggregates formed as a result of unordered collisions (random aggregation). Molecular mass (M) and effective radius (R) of aggregates formed in such a manner are related as follows: $M \sim R^{d_f}$. In the case of the DLCA regime there is a universal value of the fractal dimension of 1.8.

Thermal aggregation of proteins is characterized by the existence of an initial stage of starting aggregate formation [8, 18, 19]; their subsequent aggregation follows the DLCA regime. Taking into consideration the latent phase of starting aggregate formation, the initial time dependence of R_h is described by the following equation:

$$R_h = R_{h,0}\left[1 + \frac{1}{t_{2R}}(t - t_0)\right], \quad (5)$$

where t_0 is duration of the latent phase and t_{2R} is time interval required for the increase in hydrodynamic radius from the value $R_{h,0}$ to the value $2R_{h,0}$. Earlier it has been shown [8, 18, 19, 29] that the initial parts of the plots demonstrating ratios between the intensity of light scattering (I) and hydrodynamic radius are linear in the case of protein aggregation, and so it is not difficult to evaluate a value of hydrodynamic radius of starting aggregates ($R_{h,0}$). The value of $R_{h,0}$ is determined as a segment cut on the abscissa axis by the linear dependence of I versus R_h. Knowing $R_{h,0}$, it is possible to calculate two other parameters (t_0 and t_{2R}) from the initial part of time dependence of R_h using Eq. (5).

In the case of the RLCA regime the dependence of R_h on time (t) exhibits exponential behavior [32-34]. During thermal aggregation of proteins such a regime is realized in the presence of chaperones, e.g. in the presence of α-crystallin [8, 18]. Taking into consideration the latent phase of starting aggregate formation, the time dependence of R_h in this case may be described by the following equation:

$$R_h = R_{h,0}\left\{\exp\left[\frac{\ln 2}{t_{2R}}(t - t_0)\right]\right\}. \quad (6)$$

After calculation of the $R_{h,0}$ parameter using the ratio between the intensity of light scattering and hydrodynamic radius, the other parameters (t_0 and t_{2R}) can be found using Eq. (6).

Using aggregation of glyceraldehyde-3-phosphate dehydrogenase it was demonstrated [20] that Eqs. (4)-(6) are applicable for studies of protein aggregation in the regime of a constant rate of temperature increase. In this case, time (t) may be substituted for temperature (T) in these equations. It should be noted that for glyceraldehyde-3-phosphate dehydrogenase the size of starting aggregates is basically temperature independent in the range of temperatures from 37 to 55°C [19, 36]. Thus it is possible to use the ratio between the intensity of light scattering and hydrodynamic radius for evaluation of the $R_{h,0}$ parameter also in the case of protein aggregation under regime of the constant rate of temperature increase.

For the DLCA regime (i.e. protein aggregation in the absence of a chaperone) Eq. (5) is replaced by the equation:

$$R_h = R_{h,0}\left[1 + \frac{1}{\Delta T_{2R}}(T - T_0)\right], \quad (7)$$

where T_0 is temperature at which appearance of starting aggregates have been registered and ΔT_{2R} is the temperature characterized by the increase in hydrodynamic radius of aggregates from the value $R_{h,0}$ to the value $2R_{h,0}$. Equation (4) is replaced by the following equation:

$$R_h = R_h^*[1 + K_1(T - T^*)]^{1/d_f}, \quad (8)$$

where R_h^* is the R_h value at $T = T^*$ and K_1 is a constant.

In the RLCA regime (i.e. protein aggregation in the presence of a chaperone) Eq. (6) is replaced by the following equation:

$$R_h = R_{h,0}\left\{\exp\left[\frac{\ln 2}{\Delta T_{2R}}(T - T_0)\right]\right\}. \quad (9)$$

Since temperature increases at a constant rate, the parameters T_0, T^*, and ΔT_{2R} can be recalculated into the parameters t_0 (duration of the latent phase resulting in starting aggregate formation), t^* (time interval at which linear time dependence of R_h is transformed into the dependence which follows the power law), and t_{2R} (the time interval characterized by the increase in hydrodynamic radius from the value $R_{h,0}$ to the value $2R_{h,0}$):

$$t_0 = (T_0 - T_{init})/v, \quad (10)$$

$$t^* = (T^* - T_{init})/v, \quad (11)$$

$$t_{2R} = \Delta T_{2R}/v, \quad (12)$$

where T_{init} is initial temperature at which heating begins and v is heating rate.

We have already demonstrated applicability of Eqs. (10)-(12) for thermal aggregation of glyceraldehyde-3-phosphate dehydrogenase in the regime of heating at a constant rate [20].

RESULTS

Study of Ph*b* aggregation using dynamic light scattering. Aggregation of Ph*b* (1 mg/ml) and the effect of α-crystallin on this process have been investigated by dynamic light scattering under conditions of temperature increase at the constant rate (1 K/min) from 25 to 70°C. Figure 1 (a and b) shows autocorrelation functions and particle size distribution for Ph*b* at several temperatures in the absence of α-crystallin. The size of protein aggregates increases with the increase in temperature. Figure 1 (c-f) shows autocorrelation functions and particle size distribution for Ph*b* in the presence of α-crystallin. In the presence of α-crystallin protein aggregates of a smaller size are formed.

Figure 2a shows more detailed information on the increase in the R_h value for Ph*b* aggregates under conditions of temperature increase in the absence and in the

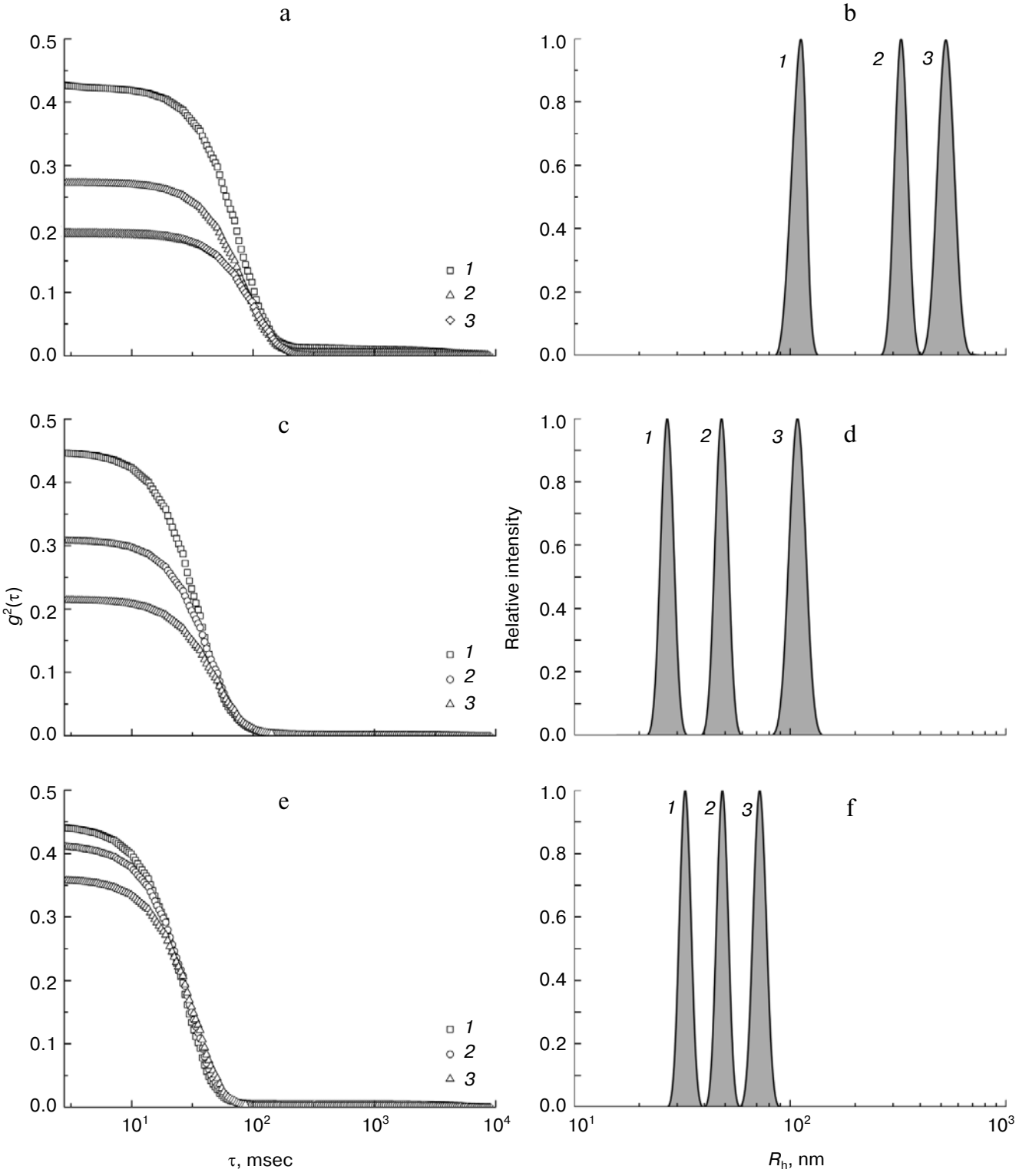

Fig. 1. Thermal aggregation of Phb (1 mg/ml) under conditions of temperature increase at the constant rate (1 K/min). Autocorrelation functions (a) and size distribution of particles (b) were obtained in the absence of α-crystallin at 50, 52, and 53°C (*1-3*, respectively). Autocorrelation functions (c) and size distribution of particles (d) were obtained in the presence of α-crystallin (1 mg/ml) at 53, 55, and 57°C (*1-3*, respectively). Autocorrelation functions (e) and size distribution of particles (f) were obtained in the presence of α-crystallin (3 mg/ml) at 57, 60, and 62°C (*1-3*, respectively). The experiments were carried out in medium containing 0.08 M Hepes, pH 6.8, 0.2 mM EDTA, and 0.1 M NaCl.

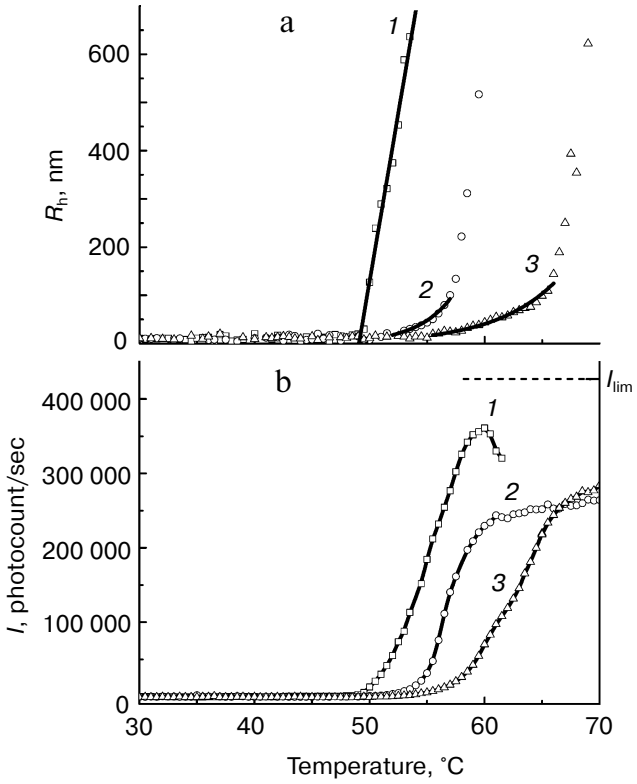

Fig. 2. Effect of α-crystallin on thermal aggregation of Ph*b* (1 mg/ml): temperature dependence of the hydrodynamic radius R_h (a) and of the intensity of light scattering I (b). The following concentrations of α-crystallin were used: 0 (*1*), 1 (*2*), and 3 mg/ml (*3*).

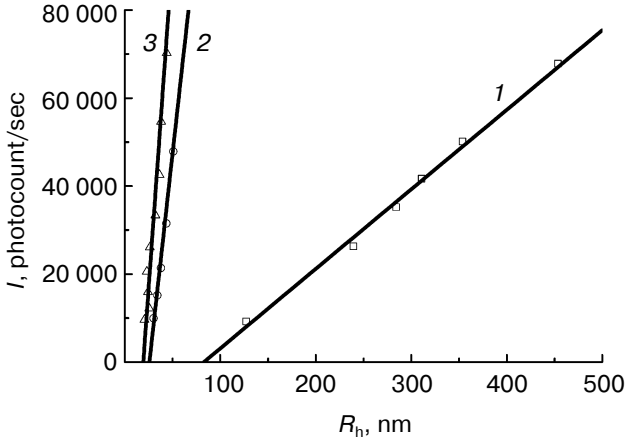

Fig. 3. Ratios between the intensity of light scattering (I) and the hydrodynamic radius R_h obtained for Ph*b* aggregation (1 mg/ml) in the absence of α-crystallin (*1*) and in the presence of 1 (*2*) and 3 mg/ml (*3*) of α-crystallin, respectively.

presence of α-crystallin. Figure 2b shows changes of the intensity of light scattering during heating of Ph*b*. Curve *1* in Fig. 2b corresponds to Ph*b* aggregation in the absence of α-crystallin. At the temperature exceeding 60°C, there was decrease in the intensity of light scattering due to precipitation of large-size protein aggregates. The presence of α-crystallin slowed the increase in light intensity with temperature and suppressed protein aggregate precipitation.

For analysis of temperature dependence of the hydrodynamic radius we have evaluated the size of the hydrodynamic radius of starting aggregates ($R_{h,0}$). We have plotted the dependences of the intensity of light scattering on the hydrodynamic radius (Fig. 3). Initial parts of these dependences are linear and a segment cut on the abscissa axis yields the value of $R_{h,0}$. In the absence of α-crystallin the $R_{h,0}$ value is 83 ± 3 nm. In the presence of α-crystallin the $R_{h,0}$ value decreases. At α-crystallin concentration of 1 and 3 mg/ml, the $R_{h,0}$ value is 26 ± 1 and 19.4 ± 0.9 nm, respectively (table).

Studying thermal aggregation of glyceraldehyde-3-phosphate dehydrogenase [11], we previously demonstrated that temperature dependence of the hydrodynamic radius includes a linear part, which is transformed into a power function. Figure 2a shows that during thermal aggregation of Ph*b* only the initial linear part of the temperature dependence of R_h (line *1*) is reliably determined. Using the determined $R_{h,0}$ value (83 ± 3 nm) and Eq. (7) it is possible to obtain the values of the parameters T_0 (the temperature corresponding to appearance of starting aggregates) and ΔT_{2R} (the time interval characterized by the increase in the hydrodynamic radius R_h from the value $R_{h,0}$ to the value $2R_{h,0}$). The parameters T_0 and ΔT_{2R} of Ph*b* aggregation in the presence of α-crystallin were determined by means of Eq. (9) and using the values of $R_{h,0}$ obtained earlier. The presence of α-crystallin caused an increase in T_0 value (table). This means that starting aggregates appear at higher temperatures. The presence of α-crystallin also causes an increase in ΔT_{2R}; this suggests deceleration of the aggregation process. It should be noted that in the case of Ph*b* aggregation in the presence of α-crystallin, free α-crystallin (possessing hydrodynamic radius of 10.5 nm) was not detected in the system. This means that α-crystallin present in the solution was totally included into protein aggregates.

The parameter T_0 can be recalculated into the parameter t_0 (the time interval required for formation of

Effect of α-crystallin on thermal aggregation of Ph*b* (1 mg/ml)

Concentration of α-crystallin, mg/ml	$R_{h,0}$, nm	T_0, °C	ΔT_{2R}, °C
0	83 ± 3	49.7 ± 0.2	0.59 ± 0.05
1	26 ± 1	53.1 ± 0.3	2.1 ± 0.2
3	19.4 ± 0.9	56.0 ± 0.4	3.7 ± 0.2

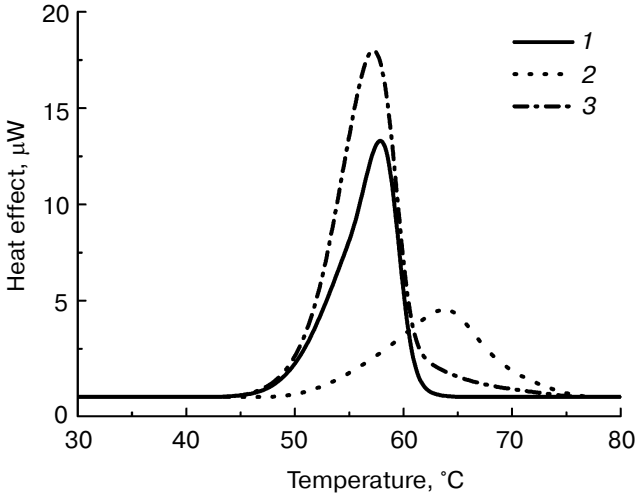

Fig. 4. Effect of α-crystallin on thermal denaturation of Ph*b* (1 mg/ml). Temperature dependences of heat absorption of Ph*b* (*1*), α-crystallin (1 mg/ml) (*2*), and the mixture of Ph*b* and α-crystallin (*3*) used in the same concentrations.

starting aggregates) using Eq. (10). In our experiments the value of T_{init} (initial temperature at which heating began) was 25°C and $v = 1$ K/min. In the absence of α-crystallin, the parameter t_0 was 24.7 ± 0.2 min. The increase in α-crystallin concentration from 1 to 3 mg/ml was accompanied by the increase in the parameter t_0 from 28.1 ± 0.3 to 31.0 ± 0.4 min, respectively.

The parameter ΔT_{2R} can be recalculated into the parameter t_{2R} (the time interval required for the increase in the hydrodynamic radius from the value $R_{h,0}$ to the value $2R_{h,0}$) using Eq. (12). In the absence of α-crystallin, the parameter t_{2R} was 0.59 ± 0.05 min. The increase in α-crystallin concentration from 1 to 3 mg/ml was accompanied by the increase in the parameter t_{2R} from 2.1 ± 0.2 to 3.7 ± 0.2 min, respectively.

Comparison of denaturation and aggregation of Ph*b*. For comparison of thermal denaturation and aggregation of Ph*b*, we have investigated enzyme denaturation by DSC. Figure 4 shows the temperature dependence of heat sorption by Phb, α-crystallin, and their mixture. In the absence of α-crystallin the denaturation profile of Ph*b* (1 mg/ml; curve *1*) is characterized by maximum at 56°C; the melting profile of α-crystallin (1 mg/ml; curve *2*) has maximum at 64°C. The denaturation profile of the mixture of these proteins is characterized by lack of a peak corresponding to free α-crystallin. The denaturation profile of the mixture of Ph*b* and α-crystallin has just one peak with maximum at 55.4°C.

For comparison of thermal denaturation and aggregation of Ph*b* we have constructed the temperature dependence Q/Q_{tot} (Q is heat sorption after reaching a certain temperature and Q_{tot} is total heat of Ph*b* denaturation) (Fig. 5a). The value of Q/Q_{tot} characterizes the proportion of denatured protein. Figure 5b shows the dependence of the intensity of light scattering on the Q/Q_{tot} value. This dependence characterizes the ratio between denaturation and aggregation of Ph*b* during heating of the enzyme (1 mg/ml) at the constant rate of 1 K/min. In the range of Q/Q_{tot} values from 0.2 to 0.8 there is a linear dependence of the intensity of light scattering on Q/Q_{tot}; thus using extrapolation it is possible to get the value of the intensity of light scattering at $Q/Q_{tot} = 1$, i.e. under conditions of total denaturation of Ph*b*. We have designated this value of the intensity of light scattering as I_{lim}. This parameter (I_{lim}) characterizes the calculated value of the intensity of light scattering under conditions of total enzyme denaturation and lack of precipitation of the formed aggregates. In Fig. 2b the level of the intensity of light scattering, which corresponds to I_{lim}, has been shown as a horizontal dashed line.

Study of oligomeric state of Ph*b* at elevated temperatures by analytical ultracentrifugation. We have earlier demonstrated that dissociation of dimeric Ph*b* into monomers occurs in the region close to maximum on the denaturation profile of this enzyme (at 53°C) [13-15]. In this study, we have controlled oligomeric state of Ph*b* at

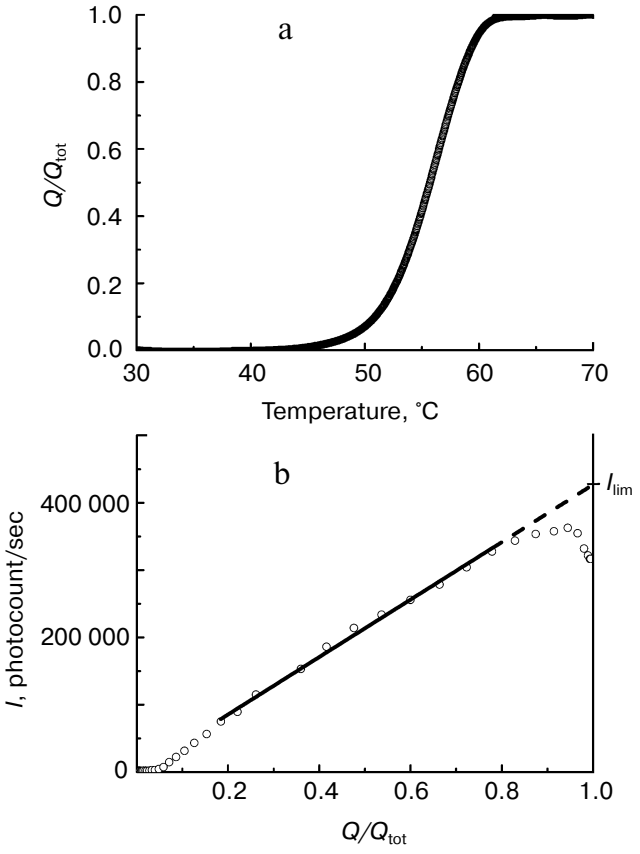

Fig. 5. Correlation between denaturation and aggregation of Ph*b* (1 mg/ml). a) Temperature dependence of Q/Q_{tot} (Q is heat absorption after reaching a certain temperature and Q_{tot} is total heat of Ph*b* denaturation). b) Dependence of the intensity of Ph*b* light scattering (I) on the Q/Q_{tot} ratio.

48°C; this corresponds to initial region of denaturation and aggregation of this enzyme. Figure 6 shows results of velocity sedimentation. During the decrease in the enzyme concentration from 1 to 0.2 mg/ml the value of the sedimentation coefficient $s_{20,w}$ of the main peak decreased from 7.0 to 5.1 S; this suggests involvement of the dissociative mechanism of thermal denaturation of Ph*b* [13-15]. We have previously demonstrated that the sedimentation coefficient of 5.1 ± 0.2 S corresponds to the monomeric form of apoPh*b* [37]. Consequently, the peak with the coefficient of 5.1 S (Fig. 6a) corresponds to the monomeric form of this enzyme. Results of our study suggest that at the enzyme concentration of 0.2 mg/ml monomeric form appears after 2.5 h and exists up to the incubation for 4 h.

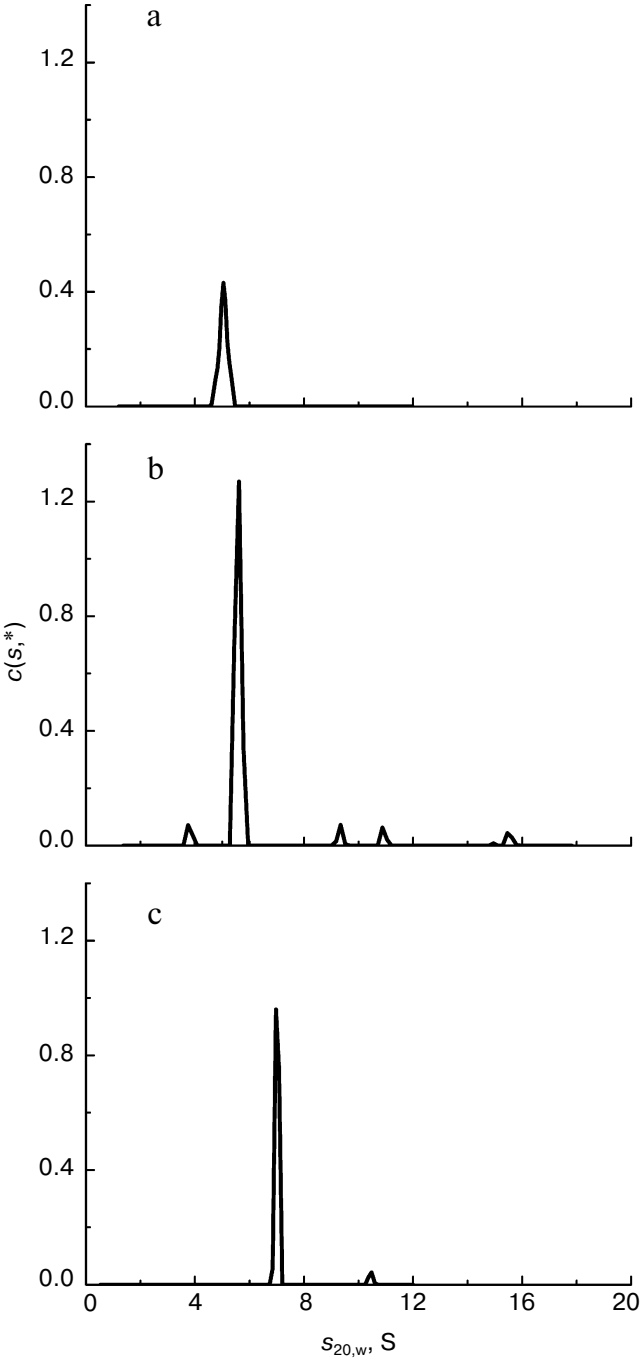

Fig. 6. Dissociation of Ph*b* during thermal denaturation. Differential distributions of the sedimentation coefficients for Ph*b* have been obtained at 48°C and normalized to the standard conditions. Total time of enzyme heating was 2 h 40 min. Concentrations of Ph*b*: 0.2 (a), 0.4 (b), and 1.0 mg/ml (c). The rotor speed was 48,000 rpm. Experiments were carried out in medium containing 0.08 M Hepes, pH 6.8, 0.2 mM EDTA, and 0.1 M NaCl.

DISCUSSION

Based on results of kinetic studies [38-43] of thermal aggregation of protein (used in a wide range of concentrations) by the turbidimetric method we have proposed a mechanism of aggregation that includes a stage of nucleation and a stage of nucleation-dependent aggregation. This mechanism has been proposed for explanation of the linear dependence of aggregation rate constant calculated from the dependence of the intensity of light scattering (or apparent absorbance) on protein concentration. Evidently, this mechanism shares similarity with the mechanism of reversible protein association, which also includes a nucleation-dependent polymerization [44].

For the aggregation mechanism involving the nucleation stage, the size of aggregates should evidently reach the limiting value during exhaustion of denatured protein. However, our subsequent studies of kinetics of thermal protein aggregation (using dynamic light scattering, which can evaluate sizes of protein aggregates) suggest that thermal aggregation of proteins is not accompanied by formation of aggregates limited in sizes. The size of aggregates constantly increased with time and reached values at which precipitation of protein aggregates began [8, 18-20, 29, 36].

Data of the present study suggest that thermal aggregation leading to formation of amorphous aggregates does not involve a stage of nucleation. It should be noted that using the turbidimetric method for registration of the aggregation kinetics the intensity of light scattering (or apparent absorbance) tend to a maximum value at rather long times. It would be reasonable to suggest that the aggregation process stops at $t \to \infty$. However, data of dynamic light scattering indicate that at the long times sticking of protein aggregates continues. This apparent discrepancy can be attributed to the fact that although large aggregates possess higher ability to scatter light, subsequent augmentation of the intensity of light scattering does not occur due to the decrease in particle number.

The results of this study on kinetics of thermal aggregation of rabbit skeletal muscle Ph*b* support a mechanism of aggregation that includes a stage of starting aggregate

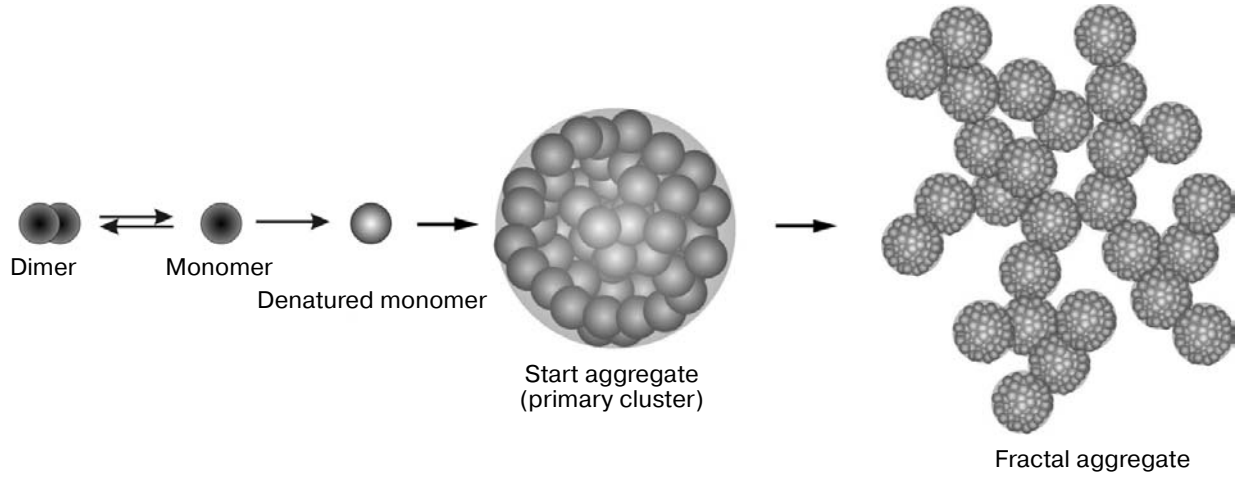

Fig. 7. Scheme of thermal aggregation of Ph*b*.

formation followed by a stage of sticking of starting aggregates and higher order aggregates. First of all, increase in temperature causes unfolding of the protein molecule. Thermal denaturation of Ph*b* occurs via the dissociative mechanism. Dissociation of native dimers of Ph*b* results in appearance of more labile monomers and therefore starting aggregates are formed from denatured monomers. Figure 7 shows a tentative scheme of denaturation and aggregation of muscle Ph*b*; it includes dissociation of enzyme dimers into monomers, formation of starting aggregates from denatured molecules, and subsequent sticking of starting aggregates.

Since initial stages of thermal aggregation of proteins include unfolding of protein molecule, the study of the effect of α-crystallin on thermal aggregation of Ph*b* has to clarify whether α-crystallin influences denaturation of this enzyme. Disappearance of the peak corresponding to free α-crystallin on the DSC curve obtained for the mixture of α-crystallin with Ph*b* and a shift of total peak to the region of lower temperatures (compared with position of peak for free Ph*b*) suggests that α-crystallin interacts with unfolding intermediates of Ph*b* molecule. A similar pattern has been observed for the effect of α-crystallin on denaturation of glyceraldehyde-3-phosphate dehydrogenase using DSC [20].

By analogy with glyceraldehyde-3-phosphate dehydrogenase, we may suggest that α-crystallin preferentially interacts with monomeric form of Ph*b* and causes shift of the monomer–dimer equilibrium towards monomer formation. Although complex formation between the monomer and α-crystallin would result in stabilization of the monomeric form, the stability of the bound monomer is lower than stability of free dimeric form of this enzyme. It should be noted that data of analytical ultracentrifugation of the mixture Ph*b* and α-crystallin at 20°C indicate that the latter does not interact with the dimeric form of Ph*b* (data not shown).

It should be noted that Rajaraman et al. [45] attributed suppression of thermal inactivation of pig mitochondrial citrate synthase (heating at 43°C) by α-crystallin to its interaction with unfolding intermediates of this enzyme.

The character of the effect of α-crystallin on thermal aggregation of Ph*b* is similar to its effect on thermal aggregation of other proteins [8, 18, 20, 36]. The presence of α-crystallin causes formation of smaller size starting aggregates. These aggregates are characterized by lower probability of sticking during their collision than starting aggregates lacking α-crystallin. This explains the decrease in the aggregation rate in the presence of α-crystallin.

In *in vitro* experiments, formation of protein aggregates is usually monitored by the increase in the intensity of light scattering (or apparent absorbance) in the visible region [6, 9, 38, 40, 41, 43]. It should be noted that when protein aggregation occurs in response to effects of various physical and chemical factors (heating, UV irradiation, moderate concentrations of chemical denaturing agents, etc.) the stage of unfolding of a protein molecule precedes the stage of aggregation. Some authors believe that turbidimetric assays can evaluate degree of protein denaturation. For example, the stability of native and glycated proteins (pig heart cytoplasmic aspartate transaminase and human serum albumin) was compared by the curves of the increase in apparent absorbance in the course of heating of protein solution at a constant rate [46-48]. For substantiation of such a conclusion, the turbidimetric assays characterizing aggregation process should be compared with the unfolding degree of protein molecule. Studying aggregation of glyceraldehyde-3-phosphate dehydrogenase during heating of protein solution in the temperature range from 40 to 67°C at a constant rate of 1 K/min, we found correlation between the intensity of light scattering and proportion

of denatured protein calculated on the basis of DSC data [18].

Levitsky at al. [49] demonstrated correlation between augmentation of the intensity of light scattering of a solution of rabbit skeletal muscle F-actin during protein heating in the range of temperatures from 30 to 70°C at the heating rate of 1 K/min and the degree of protein denaturation evaluated by DSC.

We also found correlation between apparent absorbance at 350 nm and proportion of denatured rabbit skeletal muscle creatine kinase heated at 50.6°C (this was noted after a lag-period on the kinetic curve of aggregation) [50].

It was interesting to determine whether correlation between denaturation and aggregation exists during the effect of elevated temperatures on muscle Ph*b*. The shape of the dependence of the intensity of light scattering (I) on the ratio Q/Q_{tot}, characterizing a proportion of denatured protein (Fig. 5) indicates that linear correlation between I and Q/Q_{tot} has been observed only for the interval of Q/Q_{tot} values ranging from 0.2 to 0.8. Lack of correlation between I and Q/Q_{tot} at $Q/Q_{tot} < 0.2$ may be explained by existence of additional stages including conformational transition of the dimeric enzyme molecule and dissociation of dimer into monomer [15], which precede the denaturation stages.

Linear behavior of the dependence of I versus Q/Q_{tot} for the interval of Q/Q_{tot} values ranging from 0.2 to 0.8 may be used for evaluation of maximum value of the intensity of light scattering (I_{lim}), which would be reached at high temperatures in the absence of precipitation of protein aggregates. Knowing the I_{lim} value we can normalize the value of the intensity of light scattering within the interval from 0 to 1.

Search of agents suppressing protein aggregation is important for solution of both biotechnological problems and also for development of drug preparations for medical treatment of diseases accompanied by accumulation of protein aggregates in the cell. However, until now the search for such agents is characterized by low effectiveness because the mechanism of protein aggregation has been unknown. Our findings in protein aggregation may quantitatively characterize effectiveness of agents suppressing protein aggregation and therefore help to select those agents that are the most promising in solution of the practical problems.

Authors thank Prof. D. I. Levitsky for valuable advice during discussion of this work.

This study was supported by the Russian Foundation for Basic Research (grant 05-04-48691a), Russian Foundation for Basic Research and Chinese State Foundation for Natural Sciences (grant 06-04-39008), the program "Molecular and Cell Biology" of the Presidium of Russian Academy of Sciences, and INTAS (grant 03-51-4813).

REFERENCES

1. Fink, A. L. (1998) *Folding Des.*, **3**, R9-R23.
2. Markossian, K. A., and Kurganov, B. I. (2004) *Biochemistry (Moscow)*, **69**, 971-984.
3. Hartl, F. U. (1996) *Nature*, **381**, 571-579.
4. Haslbeck, M. (2002) *Cell Mol. Life Sci.*, **59**, 1649-1657.
5. Ganea, E. (2001) *Curr. Prot. Pept. Sci.*, **2**, 1-21.
6. Horwitz, J. (1992) *Proc. Natl. Acad. Sci. USA*, **89**, 10449-10453.
7. Abgar, S., Vanhoudt, J., Aerts, T., and Clauwaert, J. (2001) *Biophys. J.*, **80**, 1986-1995.
8. Khanova, H. A., Markossian, K. A., Kurganov, B. I., Samoilov, A. M., Kleimenov, S. Yu., Levitsky, D. I., Yudin, I. K., Timofeeva, A. C., Muranov, K. O., and Ostrovsky, M. A. (2005) *Biochemistry*, **44**, 15480-15487.
9. Wang, K., and Spector, A. (1994) *J. Biol. Chem.*, **269**, 13601-13608.
10. Surewicz, W. K., and Olesen, P. R. (1995) *Biochemistry*, **34**, 9655-9660.
11. Augusteyn, R. C. (2004) *Clin. Exp. Optom.*, **87**, 356-366.
12. Barford, D., and Johnson, L. H. (1989) *Nature*, **340**, 609-616.
13. Kornilaev, B. A., Kurganov, B. I., Eronina, T. B., Chebotareva, N. A., Livanova, N. B., Orlov, V. N., and Chernyak, V. Ya. (1997) *Mol. Biol. (Moscow)*, **31**, 98-107.
14. Kurganov, B. I., Kornilaev, B. A., Eronina, T. B., Livanova, N. B., Chebotareva, N. A., Orlov, V. N., and Chernyak, V. Ya. (1997) *Proc. Int. Symp. Dedicated to 90th Anniversary of Academician N. M. Sisakyan* (Gazenko, O. G., and Poglazov, B. F., eds.) Joint Institute of Nuclear Studies, Dubna, Vol. 1, pp. 173-189.
15. Kurganov, B. I., Kornilaev, B. A., Chebotareva, N. A., Malikov, V. P., Orlov, V. N., Lyubarev, A. E., and Livanova, N. B. (2000) *Biochemistry*, **39**, 13144-13152.
16. Eronina, T. B., Chebotareva, N. A., and Kurganov, B. I. (2001) *Biochemistry (Moscow)*, **66**, 449-455.
17. Eronina, T. B., Chebotareva, N. A., and Kurganov, B. I. (2005) *Biochemistry (Moscow)*, **70**, 1020-1026.
18. Markossian, K. A., Kurganov, B. I., Levitsky, D. I., Khanova, H. A., Chebotareva, N. A., Samoilov, A. M., Eronina, T. B., Fedurkina, N. V., Mitskevich, L. G., Merem'yanin, A. V., Kleymenov, S. Yu., Makeeva, V. F., Muronetz, V. I., Naletova, I. N., Shalova, I. N., Asryants, R. A., Schmalhausen, E. V., Saso, L., Panyukov, Yu. V., Dobrov, E. N., Yudin, I. K., Timofeeva, A. C., Muranov, K. O., and Ostrovsky, M. A. (2006) *Protein Folding: New Research* (Obalinsky, T. R., ed.) Nova Science Publishers Inc, New York, pp. 89-171.
19. Markossian, K. A., Khanova, H. A., Kleimenov, S. Yu., Levitsky, D. I., Chebotareva, N. A., Asryants, R. A., Muronetz, V. I., Saso, L., Yudin, I. K., and Kurganov, B. I. (2006) *Biochemistry*, **45**, 13375-13384.
20. Khanova, H. A., Markossian, K. A., Kleimenov, S. Yu., Levitsky, D. I., Chebotareva, N. A., Golub, N. V., Asryants, R. A., Muronetz, V. I., Saso, L., Yudin, I. K., Muranov, K. O., Ostrovsky, M. A., and Kurganov, B. I. (2007) *Biophys. Chem.*, **125**, 521-531.
21. Chiou, S. H., Azari, P., Himmel, M. E., and Squire, P. G. (1979) *Int. J. Pept. Protein Res.*, **13**, 409-417.
22. Fisher, E. H., and Krebs, E. G. (1962) *Meth. Enzymol.*, **5**, 368-373.

23. Kastenschmidt, L. L., Kastenschmidt, J., and Helmreich, E. (1968) *Biochemistry*, **7**, 3590-3607.
24. Putilina, T., Skouri-Panet, F., Prat, K., Lubsen, N. H., and Tardieu, A. (2003) *J. Biol. Chem.*, **278**, 13747-13756.
25. Privalov, P. L., and Potekhin, S. A. (1986) *Meth. Enzymol.*, **134**, 4-51.
26. Yudin, I. K., Nikolaenko, G. L., Kosov, V. L., Agayan, V. A., Anisimov, M. A., and Sengers, J. V. (1997) *Int. J. Thermophys.*, **18**, 1237-1248.
27. Schuck, P. (2000) *Biophys. J.*, **78**, 1606-1619.
28. Brown, P. H., and Schuck, P. (2006) *Biophys. J.*, **90**, 4651-4661.
29. Panyukov, Y. V., Yudin, I. K., Drachev, V. A., Dobrov, E. N., and Kurganov, B. I. (2007) *Biophys. Chem.*, **127**, 9-18.
30. Elimelech, M., Gregory, J., Jia, X., and Williams, R. A. (1995) *Particle Deposition and Aggregation*: *Measurement*, *Modeling and Simulation*; Butterworth-Heinemann Ltd., Boston.
31. Jullien, R., and Botet, R. (1987) *Aggregation and Fractal Aggregates*, World Scientific Publishing Co. Pte. Ltd., Singapore.
32. Weitz, D. A., Huang, J. S., Lin, M. Y., and Sung, J. (1985) *Phys. Rev. Let.*, **54**, 1416-1419.
33. Weitz, D., and Lin, M. (1986) *Phys. Rev. Lett.*, **57**, 2037-2040.
34. Lin, M., Linsday, H., Weitz, D., Ball, R., Klein, R., and Meakin, P. (1989) *Proc. R. Soc. Lond. A*, **423**, 71-87.
35. Berka, M., and Rice, J. A. (2005) *Langmuir*, **21**, 1223-1229.
36. Khanova, E. A. (2006) *The Mechanism of Suppression of Protein Aggregation by α-Crystallin*: Candidate's dissertation [in Russian], Bach Institute of Biochemistry, Moscow.
37. Gunar, V. I., Sugrobova, N. P., Chebotareva, N. A., Stepanova, S. V., Poznanskaya, A. A., and Kurganov, B. I. (1991) in *Enzymes Dependent on Pyridoxal Phosphate and Other Carbonyl Compounds as Cofactors* (Fukui, T., Kagamiyama, H., Soda, K., and Wada, H., eds.) Pergamon Press, Oxford, pp. 417-419.
38. Kurganov, B. I. (2002) *Biochemistry (Moscow)*, **67**, 409-422.
39. Kurganov, B. I., Rafikova, E. R., and Dobrov, E. N. (2002) *Biochemistry (Moscow)*, **67**, 525-533.
40. Kurganov, B. I. (2002) *Tsinghua Sci. Technol.*, **7**, 331-339.
41. Kurganov, B. I. (2002) *Usp. Biol. Khim.*, **42**, 89-138.
42. Wang, K., and Kurganov, B. I. (2003) *Biophys. Chem.*, **106**, 97-109.
43. Kurganov, B. I. (2005) in *Chemical and Biological Kinetics. New Horizons. Vol. 2. Biological Kinetics* (Burlakova, E. B., and Varfolomeev, S. D., eds.) Koninklijke Brill NV, Leiden, The Netherlands, pp. 251-279.
44. Oosawa, F., and Kasai, M. (1962) *J. Mol. Biol.*, **4**, 10-21.
45. Rajaraman, K., Raman, B., Ramakrishna, T., and Rao, C. M. (2001) *FEBS Lett.*, **497**, 118-123.
46. Seidler, N. W., and Seibel, I. (2000) *Biochem. Biophys. Res. Commun.*, **277**, 47-50.
47. Yeargans, G. S., and Seidler, N. W. (2003) *Biochem. Biophys. Res. Commun.*, **300**, 75-80.
48. Ali Khan, M. V., Rasheed, Z., Ali Khan, V., and Ali, R. (2007) *Biochemistry (Moscow)*, **71**, 146-152.
49. Pivovarova, A. V., Mikhailova, V. V., Chernik, I. S., Chebotareva, N. A., Levitsky, D. I., and Gusev, N. B. (2005) *Biochem. Biophys. Res. Commun.*, **331**, 1548-1553.
50. Fedurkina, N. V., Belousova, L. V., Mitskevich, L. N., Zhou, H.-M., Chang, Z., and Kurganov, B. I. (2006) *Biochemistry (Moscow)*, **71**, 325-331.